ELSEVIER

Journal of Nuclear Materials 247 (1997) 151–157

journal of nuclear materials

Thermodynamics of carbothermic synthesis of actinide mononitrides

Toru Ogawa *, Yoshiro Shirasu, Kazuo Minato, Hiroyuki Serizawa

Japan Atomic Energy Research Institute, Tokai-mura, Naka-gun, Ibaraki-ken 319-11, Japan

Abstract

Carbothermic synthesis will be further applied to the fabrication of nitride fuels containing minor actinides (MA) such as neptunium, americium and curium. A thorough understanding of the carbothermic synthesis of UN will be beneficial in the development of the MA-containing fuels. Thermodynamic analysis was carried out for conditions of practical interest in order to better understand the recent fabrication experiences. Two types of solution phases, oxynitride and carbonitride phases, were taken into account. The Pu–N–O ternary isotherm was assessed for the modelling of M(C, N, O). With the understanding of the UN synthesis, the fabrication problems of Am-containing nitrides are discussed. © 1997 Elsevier Science B.V.

1. Introduction

Nitride fuels have been fabricated by carbothermic reduction of the oxides in nitrogen atmospheres [1–8]. The process will be further applied to the fabrication of nitride fuels containing minor actinides (MA: Np, Am and Cm). Already small-scale preparation has been made for neptunium nitride, NpN [9,10]. Imoto and Stoecker [11] have made a thermodynamic analysis of the equilibria of the U–C–N–O system. Their analysis have been supplemented both theoretically [12] and experimentally [13,14]. Lindemer [13] pointed out an important role of HCN and the existence of oxynitride ($UO_{2-Y}N_{3Y/4}$) as an intermediate product. In fabricating UN and (U, Pu)N, it is the practice (1) to mix carbon in a slight excess and (2) to add hydrogen to nitrogen at a certain stage of the reaction. Hydrogen promotes the reaction between carbon and oxides and also facilitates the removal of residual carbon. The aim of this study is to define the pertinent reactions and their practical implications as a basis for further process optimization. One may use nitrogen-free atmosphere in the initial stage of the heating to form the oxycarbide phase first [7]. The oxycarbide is then reacted with nitrogen to form the nitride. This route is not discussed below, because it would be hard to use this route for the fabrication of the americium-containing nitrides due to a smaller thermodynamic stability of amercium carbide.

2. Analysis

Equilibria were calculated with a Gibbs free energy minimizer ChemSage [15]. Some pertinent data are summarized and references are given in Appendix A. There are two solution phases to be considered: oxynitride and carbonitride. Uranium oxynitride, $UO_{2-Y}N_{3Y/4}$, was treated with a model by Lindemer [16]: The oxynitride is regarded as an ideal solution of UO_2 and a hypothetical $U_{4/3}N_2$. The carbonitride dissolves oxygen: The M(C, N, O) is regarded as a solution of MC, MN and a hypothetical component MO [12]. Although Potter and Spear [12] questioned the solubility data of oxygen in PuN [17], a moderate solubility of 13 ± 3 mol% PuO in PuN at 1923 K has been recently confirmed by Jain and Ganguly [18].

---

* Corresponding author. Tel.: +81-29 282 5430; fax: +81-29 282 6097; e-mail: ogawa@sun2sar.tokai.jaeri.go.jp.

PII S0022-3115(97)00041-X

One wishes to know, for instance, what would occur when adding a given amount of nitrogen to a mixture of an oxide and carbon. Because of the existence of solution phases it is necessary to follow the change of compositions of those phases and accordingly the change of activities and partial pressures with time. For this purpose, stability diagrams were calculated.

The following lists give the notation adopted in this study.

⟨ ⟩: solid species of invariant composition.
[ ]: component of a solid solution phase.
(): gaseous species.
a: thermodynamic activity.
p^*: partial pressure in MPa divided by the standard-state pressure, 0.101 MPa.
R: gas constant, 8.314 J/K · mol.
T: temperature (K).
X: molar fraction of a component in a solution.
ΔG_{f°: free energy of formation (J/mol).

3. Results and discussion

3.1. Carbothermic synthesis of UN

Fig. 1 shows parts of the stability diagram of U–C–N–O system as a function of a(C) and $p^*(O_2)$. It is calculated at $T = 1823$ K and arbitrary partial pressures of $p^*(N_2) = 0.92$ and 0.01. The boundary between the two solution phases is

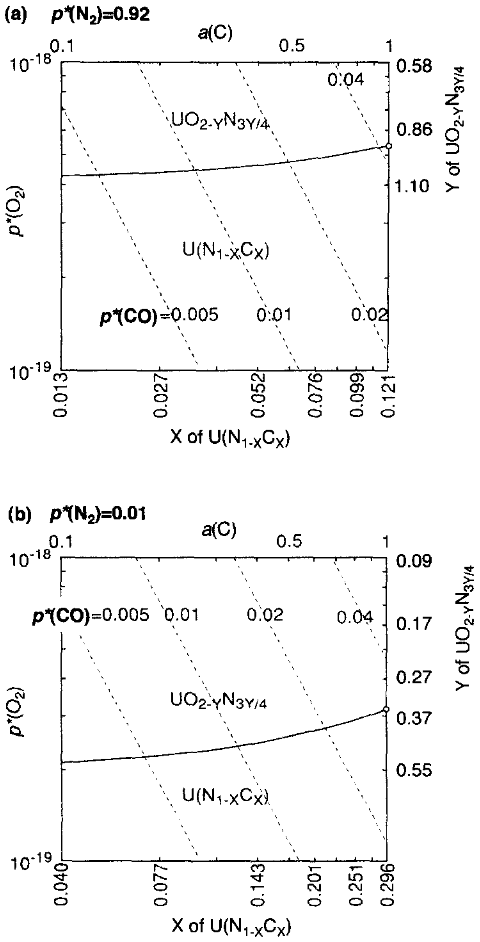

Fig. 1. Stability diagram of U–C–N–O system at 1823 K. Cross sections at (a) $p^*(N_2) = 0.92$ and (b) $p^*(N_2) = 0.01$ are shown.

given as a solid line. An open circle defines the triple point, where the oxynitride, the carbonitride and free carbon are in equilibrium. In the figures, the compositions of $UO_{2-Y}N_{3Y/4}$ and $UN_{1-X}C_X$ are indicated along an ordinate and an abscissa, respectively. The O/U of the oxynitride is independent of a(C) and the C/U of the carbonitride is rather insensitive to $p^*(O_2)$. With $p^*(N_2) = 0.92$, $UO_{1.072}N_{0.696}$, $UN_{0.878}C_{0.121}O_{0.001}$ and C are in equilibrium at the triple point; the nitrogen content in both the oxynitride and the carbonitride decreases with decreasing $p^*(N_2)$. Equilibrium $p^*(CO)$ is also shown (dashed line). One reads from Fig. 1 that, (1) $p^*(CO)$ at the triple point is 0.043 for $p^*(N_2) = 0.92$ and that (2) with the reduction of the carbon content in the carbonitride to the level of 600 ppm (C/U ~ 0.013), $p^*(CO)$ decreases by a factor of ten from that at the triple point.

One may conceptually divide the formation of UN into three stages.

(i) The conversion of UO_2 into $UO_{2-Y}N_{3Y/4}$,

$$[UO_2] + 2\langle C\rangle + (3/4)(N_2) = (3/4)[U_{4/3}N_2] + 2(CO). \tag{1}$$

(ii) the conversion of $UO_{2-Y}N_{3Y/4}$ to UC_XN_{1-X} at the triple point,

$$[UO_2] + 2\langle C\rangle + (1/2)(N_2) = [UN] + 2(CO), \tag{2}$$

$$[U_{4/3}N_2] = (4/3)[UN] + (1/3)(N_2), \tag{3}$$

$$[UN] + \langle C\rangle = [UC] + (1/2)(N_2). \tag{4}$$

(iii) The reaction of $UO_{2-Y}N_{3Y/4}$ and UC_XN_{1-X} along the boundary (solid line in Fig. 1),

$$[UO_2] + 2[UC] + (3/2)(N_2) = 3[UN] + 2(CO). \tag{5}$$

There is another route to reduce the carbon content in the carbonitride. With a substantial excess of carbon in the initial mixture, one may obtain a mixture of the carbonitride and free carbon without the oxide nor oxynitride phase. Then one may add hydrogen to nitrogen to remove free carbon. Eventually combined carbon may be also removed by the reaction

$$[UC] + (1/2)H_2 + (N_2) = [UN] + (HCN). \tag{6}$$

For the reason discussed in the introduction, regarding the stability of americium carbide, this route is not further considered in this study.

With $p^*(CO)$ derived for the above reactions, we can estimate the thermodynamic limit for the rate of reduction of total O/U and C/U ratios in flowing nitrogen. When N_2 is the major gaseous component and there is negligible partial pressure gradient, the change of total carbon content, dZ(C), is given for a given rate of nitrogen supply, d$Z(N_2)$:

$$-\mathrm{d}Z(C) = p^*(CO)\mathrm{d}Z(N_2). \tag{7}$$

Numerical integration of Eq. (7) gives the amount of carbon removed for a given cumulative nitrogen supply.

In the actual cases, however, there are significant deviations from such a simple picture. The overall reaction tends to follow the rate equation of the type

$$\ln(1 - A) = -kt, \tag{8}$$

where A is the reaction ratio (weight loss at time t divided by the total weight loss at the completion of reaction) and k the rate constant. Eq. (8) gives decreasing CO evolution rate with time, which is contrary to the simple thermodynamic prediction with Eq. (7), which gives a nearly constant rate for the initial two stages (i) and (ii). The $p^*(CO)$ does not change significantly for the most part of stage (i) and it is constant for stage (ii).

The initial mass consists of physically blended particles of the oxide and carbon, and the reaction should be controlled by the finite rate of mass transport. A series of diffusion layers or a mixture of those series should be formed. Each series of diffusion layers satisfies the local equilibrium conditions. There may be

$$/UO_2\text{-}UO_{2-Y}N_{3Y/4}/C/N_2,$$

$$/UO_2\text{-}UO_{2-Y}N_{3Y/4}/UC_XN_{1-X}(O) + C/N_2,$$

$$/UO_2\text{-}UO_{2-Y}N_{3Y/4} + C/UC_XN_{1-X}(O)/N_2,$$

$$/UO_2\text{-}UO_{2-Y}N_{3Y/4}/UC_XN_{1-X}(O)\text{-}UC_{X'}N_{1-X'}(O)/C/N_2,$$

etc., where the notation (/) indicates the boundary and (-) a series of solid solutions. The reacting components become physically separated from each other.

The oxynitride decomposes to UO_2 and U_2N_3 at lower temperatures. However, neither $UO_{2-Y}N_{3Y/4}$ nor U_2N_3 has been normally identified in the products presumably for the following reasons. The surface of UO_2 particles would be initially in direct contact with carbon, and soon covered with the carbonitride layer. Then, $p^*(N_2)$ for the interior should become

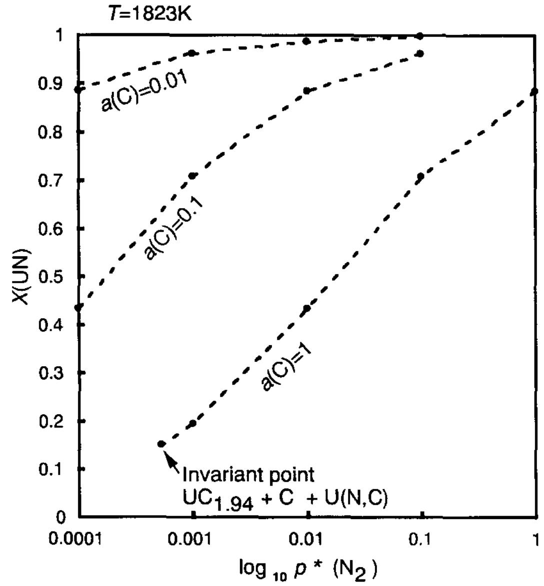

Fig. 2. Molar fraction of UN, X(UN), in U(C, N) as a function of $p^*(N_2)$ and a(C) at 1823 K.

significantly lower than that in the atmosphere. The composition gradient in the carbonitride layer is a function of $p^*(N_2)$ and a(C) (Fig. 2). By comparing Fig. 1(a) and (b), one may infer that the nitrogen content (right ordinate of the figures) in the oxynitride, which is in equilibrium with the carbonitride, decreases with decreasing $p^*(N_2)$. The carbonitride layer, however, may have fissures, or it may incompletely cover the surface of the oxide particle. Otherwise the carbon transport to the oxide component via the gas phase as discussed below will be impossible. These complexities prevent us from uniquely defining the sequence of diffusion layers.

In practice the loss of direct physical contact has been compensated by using $N_2 + H_2$ gas. As pointed out by Lindemer [13] and confirmed by Bardelle and Warin [8], carbon is efficiently transported as HCN to the oxide component. The role of HCN is catalytic in a sense, as Eq. (4), for instance, can be formally modified:

$$[UO_2] + 2\langle C\rangle + (H_2) + (3/2)(N_2) = [UO_2] + 2(HCN) + (1/2)(N_2) = [UN] + 2(CO) + (H_2) + (N_2). \quad (4')$$

However, this reaction should be written in two parts:

$$2\langle C\rangle + (H_2) + (N_2) = 2(HCN), \quad (4'')$$

$$[UO_2] + 2(HCN) = [UN] + 2(CO) + (H_2) + (1/2)(N_2). \quad (4''')$$

since, in reality, $p^*(HCN)$ over free carbon (Eq. (4″)) would differ from that over the oxynitride or oxide (Eq. (4‴)). In other words, a significant portion of free carbon can be exhausted from the system as HCN without being involved in the reactions to produce UN. Hence, carbon has to be initially in excess not only to facilitate the physical contact between carbon and the other species, but also to compensate for the loss as HCN.

Even in stage (iii) where the reaction of $UO_{2-Y}N_{3Y/4}$ and UC_XN_{1-X} occurs, the presence of HCN would give an additional route for the reaction. Besides Eq. (5) we will have

$$3[UC] + (3/2)(H_2) + 3(N_2) = 3[UN] + 3(HCN), \quad (5')$$

$$[UO_2] + 3(HCN) = [UC] + 2(CO) + (3/2)(H_2) + (3/2)(N_2). \quad (5'')$$

The $p^*(HCN)$ for Eq. (5′) is not so high:

$$p^*(HCN) = 0.052 p^*(H_2)^{1/2} p^*(N_2) a(UC)/a(UN) \sim 0.015 a(UC) = 0.015 X(UC),$$

with $p^*(N_2) \sim 1$ and $p^*(H_2) \sim 0.08$ at 1823 K. Still it would be enough for the gas-phase transport from the surfaces of UC_XN_{1-X} to $UO_{2-Y}N_{3Y/4}$. One obtains for Eq. (5″)

$$p^*(CO) = 23\{p^*(HCN) \text{ over } UO_{2-Y}N_{3Y/4}\}.$$

Thus, efficient reduction of both C and O from the system can be expected.

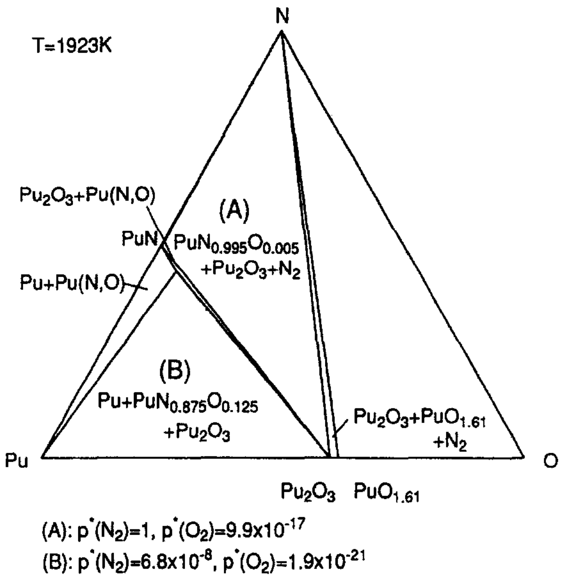

Fig. 3. Calculated Pu–N–O ternary isotherm at 1923 K.

3.2. Carbothermic synthesis of PuN and AmN

Relevant thermodynamic data are ill defined for analyzing the synthesis of PuN and AmN. Those for the americium carbide and nitride are almost absent except for an estimate for Am_2C_3 [19] and a crude assessment for AmN based on the vaporization behavior of impurity Am from a reactor grade plutonium nitride [20]: ΔG_{f° (AmN) does not appear to be so different from those of UN and PuN. On the other hand, it appears that ΔG_{f° of the carbides decreases with increasing atomic number of the actinide elements.

There is only one compound, PuN, in the Pu–N system and the same could be assumed for the Am–N system. Smaller thermodynamic stability of the carbides and the absence of the sesquinitrides make the analysis of the carbothermic synthesis of PuN and AmN simpler than that of UN. As a result, we would see that the sesquioxide is in equilibrium with the nitride which dissolves an insignificant amount of carbon. For instance, at 1673 K and $p^*(N_2) = 0.1$, $PuN_{0.996}O_{0.002}C_{0.002}$ is in equilibrium with Pu_2O_3 and C at the triple point.

Another significant difference between UN and PuN is the solubility of oxygen. Fig. 3 shows the Pu–N–O isotherm at 1923 K, which was calculated with the thermodynamic data in Appendix A. At the invariant point Pu + Pu_2O_3 + Pu(N, O), PuO dissolves in PuN to 12–13 mol%. In the products of usual carbothermic reduction, however, one would not see Pu(N, O) with such a large oxygen content. $p^*(N_2)$ is a mere $\sim 7 \times 10^{-8}$ over Pu + Pu_2O_3 + Pu(N, O), which is much smaller than the nitrogen partial pressure normally adopted for the process.

There are some notable features predicted for the carbothermic synthesis of AmN. Since Am_2O_3 is more stable than UO_2 and Pu_2O_3, $p^*(CO)$ is rather low over the mixture Am(N, O, C) + Am_2O_3 + C. The predicted $p^*(CO)$ over the three-phase mixture is ~ 0.001 at 1673 K and $p^*(N_2) = 0.1$, which is lower by a factor of six than that over U(N, C, O) + $UO_{2-Y}N_{3Y/4}$ + C under the same condition. At the same time, $p^*(Am)$ is rather high: $\sim 10^{-6}$. A low $p^*(CO)$ and a rather high $p^*(Am)$ make the carbothermic synthesis of Am-containing nitrides more difficult compared with UN and PuN.

Appendix A

Thermodynamic data of pure substances were mostly obtained from a computerized database, SGTE database [21], supplemented with the species of interest in the nuclear technology. The database is linked by a program to the Gibbs free energy minimizer ChemSage. By choosing elements and selecting pertinent chemical species from a list which the program provides to the user, necessary information such as the Gibbs energy equations and the stoichiometry coefficients is automatically organized as an input data file to ChemSage. The species taken into account in this analysis and their data origin are summarized in Table 1. The data used for the solution phases are summarized in Table 2. The parameters for $UO_{2-Y}N_{3Y/4}$ is valid only for the UO_2-rich region of the oxynitride [16]. The non-zero Redlich–Kister parameter for UC–UO pair is as estimated by Potter and Spear [12], but the Gibbs energy, G°, of UO was adjusted in accordance to G° of

Table 1
Data origin of stoichiometric pure substances considered in this study

Gas phase		Stoichiometric condensed phase	
substance	Ref.	substance	Ref.
U(G)	[21]	C	[21]
UO_3(G)	[22]	U	[21]
UO_2(G)	[22]	UO_2	[23]
UO(G)	[22]	$UN_{1.54}$	[24]
Pu(G)	[21]	U_2C_3	[20]
PuO(G)	[22]	$UC_{1.94}$	[20]
Am(G)	[23]	Pu	[21]
HCN	[21]	Pu_2O_3	[22]
CO_2	[21]	PuO_2	[21]
CO	[21]	$PuO_{1.61}$	[22]
CH_4	[21]	$PuC_{1.5}$	[21]
CH_3	[21]	Am	[23]
H_2O	[21]	AmO_2	[22]
H_2	[21]	Am_2O_3	[22]
N_2	[21]	Am_2C_3	[20]
O_2	[21]		

the other components. The G° of PuO and related non-zero Redlich–Kister parameters were fitted to the phase diagram information on Pu–C–O [12,27] and Pu–N–O [12,17,18] systems. The parameters for Am–N–C–O are very tentative in nature. They are chosen so as to represent the qualitative trend with increasing atomic number of the actinides.

Table 2
Gibbs energy parameters, G° (J/mol) = $A + B + T + CT \ln T + DT^2 + ET^3 + FT^{-1}$ and Redlich–Kister parameters of solid solutions. For the Redlich–Kister parameters, only non-zero values are shown; otherwise the parameters are set to be zero

Gibbs energy parameters

component	temperature (K)	$A \times 10^{-3}$	B	C	$D \times 10^3$	$E \times 10^8$	$F \times 10^{-5}$	Ref.
U(C, N, O)								
UC	298–2798	−117.83	346.66	−59.894	0.634	−73.3	4.4	[21]
UN	298–3000	−307.23	270.58	−48.880	−5.559	–	2.1	[25]
UO	1408–2073	−526.28	384.59	−65.474	−0.596	0.7	2.6	
$UO_{2-Y}N_{3Y/4}$								
UO_2	1000–1500	−1109.16	419.84	−72.966	−6.091	15.2	–	[22,26]
	1500–2000	−1445.41	2810.82	−398.562	134.613	−1130.1	653.5	
$U_{4/3}N_2$		−340.28	421.17	−86.098	−12.525	0.0	10.9	[a]
(Pu,Am) (C,N,O)								
$PuC_{0.88}$	298–1673	−72.29	341.62	−59.878	−2.146	17.4	9.4	[27]
PuN	298–2200	−316.48	272.81	−50.626	−5.335	–	2.6	[25]
PuO	298–1673	−562.62	322.72	−59.072	−0.596	0.7	2.6	
AmC		−39.75	324.50	−56.955	−2.439	19.8	10.7	
AmN		−314.19	249.35	−44.112	−12.843	423.6	1.7	[20]
AmO		−566.20	314.43	−58.654	−0.596	0.7	2.6	

Non-zero Redlich–Kister parameters

Component pair	L (J/mol)
UC–UO	−83680
$PuC_{0.88}$–PuO	−30000
PuN–PuO	30000
AmN–AmO	30000

[a] Value in Ref. [13] was corrected for the difference in the Gibbs energy of UO_2.

References

[1] T. Muromura, H. Tagawa, J. Nucl. Mater. 71 (1977) 65.
[2] T. Muromura, H. Tagawa, J. Nucl. Mater. 80 (1979) 330.
[3] R.B. Matthews, K.M. Chidester, C.W. Hoth, R.E. Mason, R.L. Petty, J. Nucl. Mater. 151 (1988) 334.
[4] G. Pautasso, K. Richter, C. Sari, J. Nucl. Mater. 158 (1988) 12.
[5] Y. Arai, S. Fukushima, K. Shiozawa, M. Handa, J. Nucl. Mater. 168 (1989) 280.
[6] S.K. Mukerjec, J.V. Dehadraya, V.N. Vaidya, D.D. Sood, J. Nucl. Mater. 185 (1991) 39.
[7] G. Ledergerber, Z. Kopajtic, F. Ingold, R.W. Stratton, J. Nucl. Mater. 188 (1992) 28.
[8] P. Bardelle, D. Warin, J. Nucl. Mater. 188 (1992) 36.
[9] Y. Arai, C. Sari, J.C. Spirlet, J. Nucl. Mater. 185 (1991) 159.
[10] Y. Suzuki, Y. Arai, Y. Okwnoto, T. Ohmichi, J. Nucl. Sci. Technol. 31 (1994) 677.
[11] S. Imoto, H.J. Stoecker, Thermodynamics, Vol. 11 (IAEA, Vienna, 1966) pp. 533–545.
[12] P.E. Potter, K.E. Spear, Thermodynamics of Nuclear Materials (IAEA, Vienna, 1979) pp. 195–227.
[13] T.B. Lindemer, J. Am. Ceram. Soc. 55 (1972) 601.
[14] A. Naoumidis, H.J. Stoecker, Thermodynamics of Nuclear Materials (IAEA, Vienna, 1976) pp. 287–300.
[15] G. Eriksson, K. Hack, Metall. Trans. B21 (1990) 1013.
[16] T.B. Lindemer, Calphad 13 (1989) 109.
[17] R. Lorenzelli, P. Delaroche, M. Housseau, P. Petit, Nucl. Metall. 17 (2) (1970) 818 (Metallurgical Society of the American Institute of Mining, Metallurgical, and Petroleum Engineers, New York).
[18] G.C. Jain, C. Ganguly, J. Nucl. Mater. 202 (1993) 245.
[19] C.R. Holley Jr., M.H. Rand, E.K. Storms, The Chemical Thermodynamics of Actinide Elements and Compounds, Part 6: The Actinide Carbide (IAEA, Vienna, 1984).
[20] T. Ogawa, T. Ohmichi, A. Maeda, Y. Arai, Y. Suzuki, J. Alloys Compounds 224 (1995) 55.
[21] P.J. Spencer et al., Swiss Chem. 12 (1990) 61.
[22] E.H.P. Cordfunke, R.J.M. Konings, Thermochemical Data for Reactor Materials and Fission Products (Elsevier, Amsterdam, 1990).
[23] F.L. Oetting, M.H. Rand, R.J. Ackermann, The Chemical Thermodynamics of Actinide Elements and Compounds, Part 1, The Actinide Elements (IAEA, Vienna, 1976).
[24] H. Tagawa, J. Nucl. Mater. 51 (1974) 78.
[25] I. Barin, Thermochemical Data of Pure Substances (VCH, Weinheim, 1989).
[26] J.K. Fink, M.G. Chasanov, L. Leibowitz, J. Nucl. Mater. 102 (1981) 17.
[27] T.M. Besman, T.B. Lindemer, J. Nucl. Mater. 67 (1977) 77.